Determination of the Solution Structure of Neuropeptide K by High-Resolution Nuclear Magnetic Resonance Spectroscopy†

James Horne,*,‡ Maruse Sadek,§ and David J. Craik‡

School of Pharmaceutical Chemistry, Victorian College of Pharmacy, Monash University, 381 Royal Parade, Parkville, Victoria 3052, Australia, and Centre for Protein and Enzyme Technology, La Trobe University, Bundoora, Victoria 3083, Australia

Received January 19, 1993; Revised Manuscript Received April 27, 1993

ABSTRACT: ^{1}H NMR chemical shift assignments for neuropeptide K (NPK) and neurokinin A (NKA) have been determined at 600 MHz in 28% trifluoroethanol/water solution. Two-dimensional NMR techniques were used to assign proton resonances, and interproton distances were estimated from the observed nuclear Overhauser effects (NOEs). These distances were used as constraints in a simulated annealing protocol within the program XPLOR to generate structures consistent with experimental data. NPK forms a regular amphipathic α-helical structure from Asp 3, terminating at Gly 18. Slowly exchanging amide protons identified in this region are likely to be involved in hydrogen bonds to stabilize the helix. The remainder of the molecule displays many sequential NOEs, with some i–(i + 2) contacts, but little further evidence of defined secondary conformation. NKA displays strong sequential connectivities between amide protons from Thr 3 to Met 10, and some i–(i + 2) connectivities suggestive of a series of dynamic turns in equilibrium. A comparison of the tail region of NPK with the related peptide homologue, neurokinin A, in the same solvent system, indicates that both show increasing order when trifluoroethanol is titrated into water solution, with the appearance of sequential NOEs between backbone amide protons. Differences between the corresponding spans of primary sequence appear to be minimal. The clear finding that NPK adopts a well-defined helix in its N-terminal half and is relatively disordered in the C-terminal half, which includes the entire NKA sequence, may have important implications for understanding the increased selectivity of NPK over NKA for one class of neurokinin receptor.

The tachykinin class of neuropeptides has been shown to exhibit a wide range of biological effects in mammals. Alterations in tachykinin distribution have been noted in conjunction with some neurological and physiological disorders, notably Parkinsonism and schizophrenia (Henry *et al.*, 1987). They have been implicated in cardiovascular, respiratory, and gastrointestinal functions and inflammatory processes (Helke *et al.*, 1990) and have putative roles in neurotransmission processes. SP, NKB, and NKA[1] are the earliest known members of the class, and all are present in mammals. They are characterized by the shared C-terminal sequence Phe-X-Gly-Leu-Met-NH_2. SP, NKA, and NKB are nominally the primary ligands for the G-protein-coupled NK-1, NK-2, and NK-3 receptors, respectively (Hanley & Jackson, 1987), though there is a high degree of cross-specificity for these ligands among the receptor classes (Holzemann, 1989). While the role of tachykinin receptor subtypes is still being clarified, there is already considerable interest in these peptides as potential targets in the design of novel drugs.

NPK is a 36 amino acid peptide, found in mammalian tissue, that contains the entire NKA sequence in its C-terminal region (Tatemoto *et al.*, 1985). NPK has been shown to inhibit binding of radiolabeled NKA to rat duodenum smooth muscle cells (rich in NK-2 receptor sites) with higher affinity than NKA (Beaujouan *et al.*, 1988). NKA and NPK are primarily selective for the NK-2 receptor site, with NPK the more potent, and either peptide can be generated from the same preprotachykinin gene through alternate tRNA transcription (Nawa *et al.*, 1983).

Recently, several studies have led to reports on biophysical properties of tachykinin neuropeptides. High-resolution NMR spectroscopy has been used to determine possible solution conformations of SP, NKA, and other analogues, either synthetic or naturally derived (Loeuillet *et al.*, 1989, Levian-Teitelbaum *et al.*, 1989). In general it has been found that tachykinins display some elements of secondary structure under appropriate solution conditions, though it has been suggested that they may undergo rapid conformational exchange (Sumner *et al.*, 1990). As such conformational variability is common for small peptides (Dyson & Wright, 1991), the increased size of NPK and its improved selectivity for the NK-2 receptor site, compared with those characteristics of NKA, made it an important target for structural investigation.

In this report we present ^{1}H NMR spectral data recorded at 600 MHz for NPK in 28% trifluoroethanol-d_3 (TFE-d_3) solution. Sequence-specific assignment of the NMR spectra is made, and experimental distance constraints are estimated from observation of nuclear Overhauser effects. The NOE data were used as input for a series of simulated annealing calculations within the molecular dynamics package XPLOR (Brunger, 1992), and potential structures were generated for the neuropeptide. The ^{1}H NMR spectrum of NKA was also

† This work was supported in part by a grant from the Australian Research Council and the Department of Employment, Education and Training.

* Author to whom correspondence should be addressed.

‡ Monash University.

§ La Trobe University.

[1] Abbreviations: DQFCOSY, double-quantum filtered correlated spectroscopy; 2D, two dimensional; NMR, nuclear magnetic resonance; TOCSY, total correlated spectroscopy; NOE, nuclear Overhauser enhancement; NOESY, nuclear Overhauser enhancement spectroscopy; ROESY, rotating-frame Overhauser enhancement spectroscopy; ECOSY, exclusive correlation spectroscopy; RMSD, root mean square deviation; NKA, neurokinin A; NPK, neuropeptide K; SP, substance P; NKB, neurokinin B; TFE, trifluoroethanol; AMX spin system containing three protons.

0006-2960/93/0432-7406$04.00/0

recorded and assigned in 28% TFE-d_3, and NOE measurements were made at 600 MHz. Distance constraints were estimated and structures generated for NKA which were then compared to the homologous region of NPK.

EXPERIMENTAL PROCEDURES

Sample Preparation. NPK for these studies was obtained from AUSPEP PTY LTD. Some preliminary experiments were carried out in 90% H_2O/10% D_2O solution with 5.0 mg of peptide in 0.45 mL, which was subsequently recovered by freeze-drying. In most experiments, an aqueous mixture of TFE-d_3 was used as a solvent. Peptide (5.0 mg) was dissolved in 0.45 mL of 28% TFE-d_3 in distilled water. The solution was transferred to a 535-PP Wilmad NMR tube, and the tube was sealed under nitrogen. The pH of this solution was measured to be 3.3 (uncorrected). A second sample in 28% TFE-d_3 in deuterium oxide was also prepared, allowing us to observe potential resistance to deuteron exchange. Only 1 mg of peptide was needed to yield adequate signal-to-noise for one-dimensional experiments in this solvent mixture. NKA was also supplied by AUSPEP. Peptide (5 mg) was dissolved in 0.45 mL of 28% TFE-d_3/H_2O and placed in a 5-mm NMR tube. The pH of this solution was measured to be 3.0 (uncorrected).

Data Acquisition. All spectra for NPK were measured on a Bruker AMX-600 spectrometer. TOCSY (mixing time 80 ms with no trim pulses) (Davis & Bax, 1985; Griesinger *et al.*, 1988), DQFCOSY (Rance *et al.*, 1983), and ECOSY (Griesinger *et al.*, 1987) experiments were collected with 16, 32, and 32 transients, respectively, and 512, 800, and 800 t_1 increments. NOESY experiments (Kumar *et al.*, 1980) were collected at 96 transients and 512 t_1 increments with mixing times of 50, 100, and 250 ms. All spectra were recorded at 298 K, with 4096 data points in F_2. The spectral width was 6097 Hz at 600 MHz.

TOCSY (80 ms) and ROESY (100 ms) (Bothner-By *et al.*, 1984) spectra for NKA were acquired on a Bruker AMX 300 spectrometer at 298 K for assignment purposes. Typically 32 transients were collected, with 512 t_1 increments over 4096 data points. Spectral width was 3030 Hz. For NOESY (250 ms) experiments with presaturation, data were acquired on the Bruker AMX 600 spectrometer for determination of secondary structure, with 80 transients and 512 t_1 increments at 278 K. Spectral width was 6097 Hz, and data were acquired with 2048 data points.

Solvent Suppression. Suppression of the H_2O resonance in NMR spectra was achieved either by selective excitation with binomial pulses in some NOESY experiments (Plateau *et al.*, 1982) or through irradiation of the solvent frequency during the recycle delay for DQFCOSY and TOCSY experiments. In both cases the solvent resonance was placed on the carrier frequency. Presaturation of solvent was achieved via a 2-s pulse at approximately 0.2 mW from the ECOUPLER unit of the Bruker AMX spectrometer. The null point of the binomial pulse was set at the solvent frequency, and the interpulse delay was set to provide maximum signal intensity at the midpoint of the backbone amide resonances.

Data Processing. Data processing was performed on a Silicon Graphics workstation using the program FELIX (Hare Research Inc.). Prior to Fourier transformation of the free induction decays (FIDs), a 70°-shifted sine bell window function was applied in both dimensions to improve resolution in overlapped spectral regions. For quantitative measurement of NOESY data, only 90°-shifted sine bells were applied to avoid distortion of volume integrals. Data were zero-filled to yield a $2048K \times 2048K$ "real" matrix with a digital resolution of 2.98 Hz/pt.

Base line correction of two-dimensional matrices was applied to improve quantitation of crosspeak volumes in NOESY spectra. This was done by fitting a third-order polynomial or cubic spline function as required, on the basis of the manual selection of true base line points in selected transformed slices of the data matrix. Half of the transformed NOESY data were multiplied by −1 to display all information in the positive plane due to phase distortion by the binomial observe pulse.

Estimation of Distance and Dihedral Constraints. Crosspeak volume integrals for clearly resolved peaks were measured from 250-ms NOESY experiments. In cases where overlap occurred, estimates of some volume integrals were made with allowance for the contribution of overlapped resonances to the observed peak intensity. Care was taken not to overinterpret the NOE intensity data, which were categorized as strong, medium, weak, and very weak corresponding to upper-bound constraint distances of 2.7, 3.5, 5.0, and 6.0 Å, respectively. These were then applied in modeling strategies with a lower-bound cutoff of the van der Waals radii. Appropriate pseudoatom corrections (Wuthrich, 1986) were added to the constraints for nonstereospecifically assigned protons and degenerate methyl and aromatic protons. A total of 235 NOE constraints were applied for NPK and 67 constraints for NKA in the subsequent simulated annealing protocol.

Dihedral angles were determined by applying a Karplus relationship (Pardi *et al.*, 1984) to the experimentally derived coupling constant information. $J_{N\alpha}$ and $J_{\alpha\beta}$ coupling constants were measured, where possible, from DQFCOSY and ECOSY experiments. Some additional $\alpha\beta$ couplings in AMX systems were inferred from the observed multiplicity of peaks from an 80-ms TOCSY experiment (Driscoll *et al.*, 1989). Dihedral constraints were not included in the structure calculation protocol but were subsequently compared with values obtained in the calculated structures.

RESULTS

Some preliminary 1D and 2D spectra of NPK were recorded in aqueous solution at 298 K. On the basis of the observation of a relatively small number of crosspeaks in NOESY spectra, it was concluded that NPK adopts essentially a random coil conformation under these conditions. Aliquots of TFE-d_3 were then added to an aqueous solution of NPK, and a series of 1D ^1H NMR spectra were recorded at 300 MHz and 298 K. At up to 28% v/v TFE/water, no significant changes were observed in these 1D spectra, primarily due to their highly overlapped nature. Many literature reports have shown secondary structural stabilization for peptides in solutions of TFE from 30% to 50% v/v in water. It was therefore decided to stop the titration at this point and record a NOESY spectrum to determine if any secondary structural stabilization was apparent. At the final proportion of 28% TFE-d_3/72% H_2O v/v, NOESY spectra indicated that secondary structural stabilization was apparent. All subsequent experiments were performed under these solution conditions.

Spectral Assignment. TOCSY and DQFCOSY experiments were used to identify most of the side chains of NPK by scrutiny of characteristic coupling patterns (Wuthrich, 1986). Alanine and threonine were readily distinguished from the larger methyl-containing residues. α and β proton chemical shifts of Thr 29 were similar, but a crosspeak due to coupling of these protons was observed in the DQFCOSY spectrum, thereby allowing unambiguous assignment. By inference, all

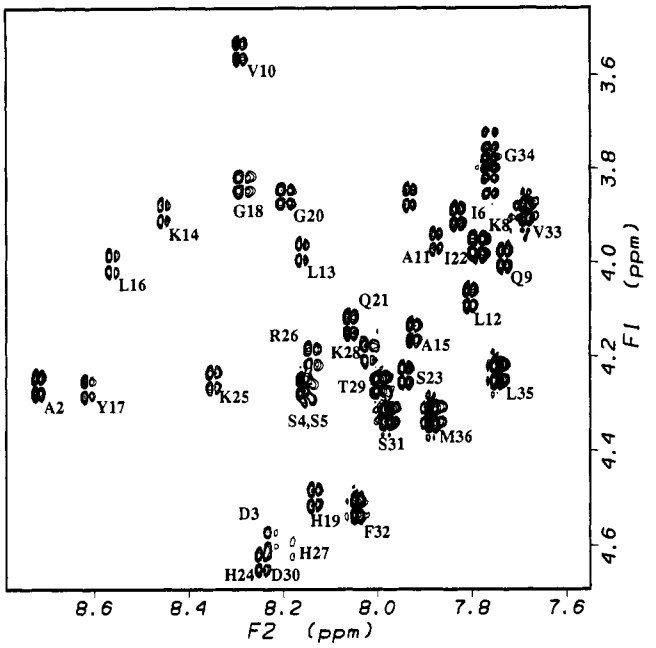

FIGURE 1: Expansion of fingerprint region of DQFCOSY spectrum for NPK in 28% TFE-d_3/water at 298 K. The sequential assignments are indicated next to the appropriate H^N–H^α crosspeaks.

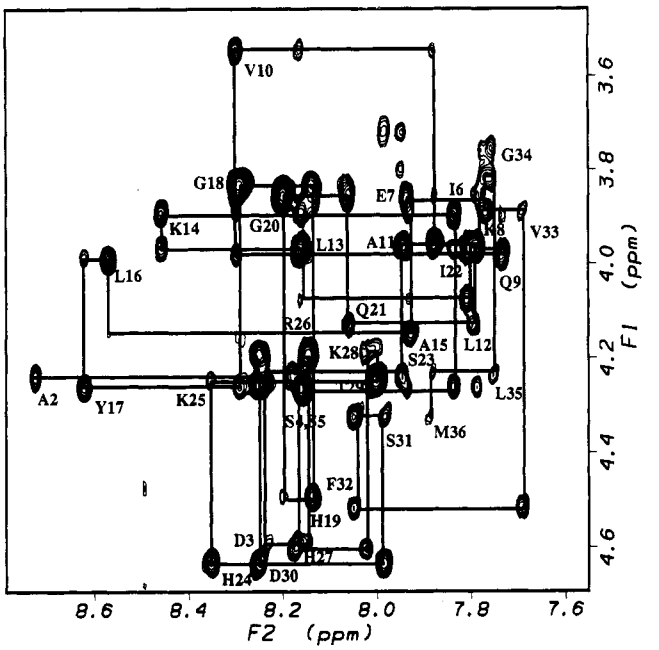

FIGURE 2: Expansion of fingerprint region of NOESY 250-ms spectrum for NPK in 28% TFE-d_3/water at 298 K. The sequential pathway is indicated by a filled line joining intraresidue to interresidue connectivities.

other single methyl-containing spin systems were attributed to alanine. Isoleucine, leucine, and valine were readily distinguishable from their coupling patterns in expansions of the aliphatic region of DQFCOSY spectra. The single arginine residue was easily found, but the four lysines were heavily overlapped with some leucine α shifts, making them difficult to discriminate. The $\beta\gamma$ systems of methionine, glutamine, and glutamate were identified but could not be assigned individually until the sequential assignment was determined. Of the many AMX spin systems, the aromatic residues tyrosine, histidine, and phenylalanine were identified on the basis of NOESY connectivities between the aromatic protons and the α or β protons. Serines were distinguished from other AMX spin systems by the characteristic low-field chemical shifts of their β protons. Glycines displayed characteristic double H^α–H^N couplings in DQFCOSY spectra, although the multiplicity was not completely observed in some cases. All other AMX systems were fully identified in the sequential assignment.

After most spin systems had been identified from DQFCOSY and TOCSY spectra, the sequence-specific assignments were made from a combination of DQFCOSY and NOESY spectra (Wuthrich, 1986). Examination of the fingerprint (i.e., H^α–H^N) region of both spectra and the H^N–H^N region of the NOESY spectrum was useful for this purpose. Figure 1 shows the fingerprint region of the DQFCOSY spectrum and illustrates that all but the first of the 36 expected connectivities between the α proton of a residue and its H^N proton are observed. In the corresponding region of the NOESY spectrum (Figure 2), additional crosspeaks connecting the H^α of one residue with the H^N proton of the next are observed. The sequential pathway connecting the crosspeaks is indicated in Figure 2. In cases where there was some ambiguity in resolving the pathway, reference was made to the H^N–H^N region of the NOESY spectrum. Table I contains the completed chemical shift assignments for NPK.

For neurokinin A, chemical shift assignments have been made previously in other solvent systems (Chassaing *et al.*, 1987) and do not deviate greatly from our own measurements in TFE-d_3 solution. These were a useful guide for making a full assignment. All spin systems could be identified in expansions of the aliphatic region of the 80-ms TOCSY spectrum at 300 MHz. Among the AMX spin systems, His

Table I: ^{1}H NMR Chemical Shifts[a] (ppm) of Neuropeptide K in 28% TFE-d_3

residue	NH	α	β	others
Asp-1				
Ala-2	8.71	4.24	1.32	
Asp-3	8.19	4.56	2.82, 2.74	
Ser-4	8.12	4.24	3.87, 3.93	
Ser-5	8.10	4.22	3.86, 3.94	
Ile-6	7.80	3.88	1.82	1.48, 1.13(γ), 1.35(δ)
Glu-7	7.90	3.83	2.03, 2.06	2.37, 2.44(γ)
Lys-8	7.74	3.94	1.83	1.60(γ), 1.36(δ), 2.85(ϵ)
Gln-9	7.70	3.96	2.10, 2.17	2.24, 2.36(γ), 6.46, 6.70(NH2)
Val-10	8.26	3.55	3.93	1.42
Ala-11	7.86	3.95	1.40	
Leu-12	7.77	4.04	1.65, 1.74	1.59(γ), 0.78, 0.81(δ)
Leu-13	8.13	3.94	1.84	1.50(γ)
Lys-14	8.42	3.87	1.76, 1.86	1.29, 1.55(γ), 1.62(δ), 2.79(ϵ)
Ala-15	7.89	4.12	1.47	
Leu-16	8.52	3.97	1.68, 1.77	1.25(γ), 0.67, 0.73(δ)
Tyr-17	8.57	4.24	2.99, 3.03	7.01(2,6H), 6.66(3,5H)
Gly-18	8.25	3.80, 3.73		
His-19	8.10	4.47	3.16, 3.34	7.22(4H), 8.47(1H)
Gly-20	8.16	3.78, 3.83		
Gln-21	8.03	4.10	1.91, 2.02	2.17(γ)
Ile-22	7.76	3.95	1.75	1.06(γ), 0.73(δ), 0.69(δ)
Ser-23	7.91	4.21	3.69, 3.77	
His-24	8.20	4.61	2.72	7.19(4H), 8.47(1H)
Lys-25	7.99	4.16	1.68, 1.74	1.31(δ)
Arg-26	8.10	4.17	1.65, 1.71	1.50, 1.55(γ), 3.06(δ)
His-27	8.14	4.56	2.82	7.19(4H), 8.47(1H)
Lys-28	8.32	4.22	1.69, 1.75	1.59(γ), 1.34(δ), 2.89(ϵ)
Thr-29	7.96	4.23	4.15	1.09(γ)
Asp-30	8.22	4.61	3.08, 3.20	
Ser-31	7.95	4.30	3.70	
Phe-32	8.01	4.47	3.15, 3.34	7.12(arom)
Val-33	7.65	3.86	1.95	0.81(γ)
Gly-34	7.73	3.73, 3.78		
Leu-35	7.72	4.20	1.49, 1.58	0.81(γ), 0.77(δ)
Met-36	7.85	4.29	1.89, 2.00	2.36, 2.45(γ)
Nterm	6.83, 7.17			

[a] Chemical shifts are expressed relative to DSS at 0.0 ppm.

Table II: ^{1}H NMR Chemical Shifts[a] (ppm) of Neurokinin A in 28% TFE-d_3

residue	NH	α	β	others
His-1	8.28	4.27		8.59(1H), 7.37(4H)
Lys-2	8.81	4.39	1.67	1.79(γ), 1.67(δ), 2.96(ϵ)
Thr-3	8.29	4.31	4.20	1.17(γ)
Asp-4	8.31	4.64	2.71	
Ser-5	8.05	4.36	3.75	
Phe-6	8.13	4.57	3.07	7.20(arom)
Val-7	7.73	3.93	2.00	0.86(γ)
Gly-8	7.79	3.85, 3.79		
Leu-9	7.80	4.28	1.60	0.86(γ)
Met-10	7.95	4.37	2.06, 1.97	2.53, 2.43(γ), 6.90, 7.24(NH_2)

[a] Chemical shifts are expressed relative to DSS at 0.0 ppm.

Chart I: Summary of NOE Data for Neuropeptide K in 28% TFE-d_3/Water at 298 K[a]

[a] The relative size of filled blocks represents the intensity of the NOE. Shaded regions indicate that estimation of peak size was impossible. Stars indicate protons resistant to deuteron exchange.

1 was identified by coupling between the H^δ aromatic proton and its β protons. Phe 6 could be identified from H^δ aromatic proton to β proton coupling in NOESY spectra and Ser 5 from the characteristic low-field chemical shift of its β protons. Asp 4 was then assigned by elimination. Lys 2, Thr 3, Val 7, Leu 9, and Met 10 were identified from relayed-type crosspeaks from their backbone amide protons in TOCSY spectra. Gly 8 displayed characteristic double H^α–H^N couplings in TOCSY spectra. The fingerprint region of the 250-ms NOESY spectrum was used to confirm the sequential assignment. Table II contains the completed chemical shift assignments for NKA.

Secondary Structural Analysis. Chart I summarizes the observed NOE information, which is useful for qualitatively identifying elements of secondary structure in the NPK sequence. The presence of a continuous sequence of strong H^N_i–H^N_{i+1} connectivities in the first half of the sequence, combined with weaker H^α_i–H^N_{i+1} connectivities and a range of appropriate medium-range linkages (i.e., H^N_i–H^N_{i+2} H^α_i–H^N_{i+3}), is suggestive of a helical structure in this region. This is supported by amide proton exchange data. Spectra of freshly prepared NPK in 28% TFE-d_3/D_2O solution revealed that Ala 11, Leu 16, Tyr 17, Gly 18, Lys 25, and Thr 29 were resistant to exchange with deuterons for a period of greater than 8 h. Resistance to exchange is indicative of solvent inaccessibility or participation in hydrogen bonding (Wuthrich, 1986).

Further support for the presence of a helical structure is found in the relative intensity ratios for intra- and interresidue H^α–H^N crosspeaks. Extended conformations generally yield strong interresidue crosspeaks and weaker intraresidue cross-

Chart II: Summary of NOE Data for Neurokinin A in 28% TFE-d_3/Water at 278 K[a]

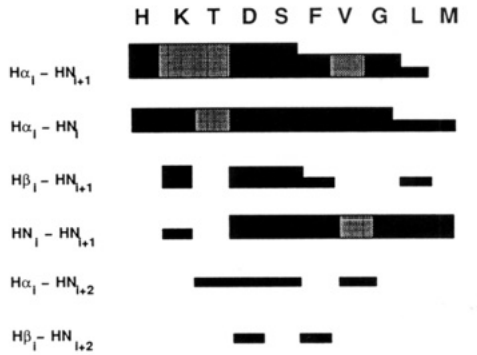

[a] The relative size of the filled blocks represents the intensity of the NOE. Shaded regions indicate that estimation of peak size was impossible.

peaks, while for helical conformations the intraresidue connections are enhanced. For the first half of the sequence of NPK, intraresidue crosspeaks are more intense. Similarly, variations in relative intensities of d^{NN} and $d^{\alpha N}$ sequential connectivities support the proposal of a helical structure (Bradley *et al.*, 1990). In the N-terminal half of NPK, the d^{NN} contacts are stronger than the $d^{\alpha N}$ contacts, which is in contrast to the C-terminal half, where the d^{NN} contacts are much weaker.

NOESY spectra of NKA obtained at 298 K and 300 MHz in 28% TFE-d_3/H_2O did not yield strong NOE crosspeaks. Such an observation could reflect either a lack of defined structure or a nulling of NOE intensity due to correlation time effects. To distinguish between these possibilities, a ROESY spectrum was recorded at this temperature and a NOESY spectrum at higher field and lower temperature. ROESY does not suffer from nulling of crosspeaks in NOESY experiments on small peptides, and with the complementary approach of increasing field and decreasing temperature we expected to significantly shift the correlation time away from the extreme narrowing limit. ROESY spectra at 298 K indicate a short run of sequential NOEs from Asp 4 to Val 7. NOESY spectra of NKA at 278 K and 600 MHz contain strong sequential H^N_i–H^N_{i+1} connectivities, which are in phase with the diagonal, in a continuous span from Lys 2 to Val 7 and from Leu 9 to Met 10. The sequence of connectivities probably includes Val 7 and Gly 8, but as the H^N protons of these residues are degenerate, this could not be established with certainty. A number of H^α_i–H^N_{i+2} and H^β_i–H^N_{i+2} linkages are observed throughout the sequence. The N-terminus is likely to be flexible, with loss of intensity noted for the histidine and lysine spin systems in TOCSY and ROESY experiments at 298 K and 300 MHz. At lower temperature the intensity of the lysine spin system noticeably increases, and line shape is sharper for the backbone amide proton. Chart II summarizes the relevant NOESY information for NKA.

Generation of Three-Dimensional Structures. Given the indication of a helical structure in at least part of the sequence of NPK, it was of interest to use the observed NOEs to obtain more quantitative structural information. This was done using a simulated annealing protocol (Nilges *et al.*, 1988) with the program XPLOR (Brunger, 1992; Brunger *et al.*, 1986). The starting structure for the protocol consisted of a template set of coordinates in which the peptide backbone was extended along the x axis, with y and z coordinates randomized. The structure was regularized to give good local geometry with no nonbonded contacts, using a short period of dynamics and subsequent energy minimization with 200 steps of the Powell algorithm. A series of 100 simulated annealing runs was then

made using the NOE constraints in combination with a modified CHARMM (Brooks *et al.*, 1983) force field. High-temperature dynamics was run for 15 ps at 2000 K, with each of the 100 calculations initiated using randomized dynamics trajectories. In the early stage of the calculations, only weak repulsive terms were in operation, effectively allowing atoms to pass through each other. A low slope (asymptote) of the NOE constraint term (a soft square well potential) was used through the initial stage and was increased during the subsequent cooling stage. The structures were annealed with 50-deg temperature steps, reaching a final temperature of 300 K. The nonbonded repulsive term was increased concommitantly with the NOE asymptote in an exponential fashion to prevent further crossing of atoms during annealing. A further 200 cycles of energy minimization yielded a set of structures which was statistically analyzed for NOE violations. Visualization of structures with INSIGHT (Biosym software) allowed populations of similar conformers to be superimposed. Within the set of structures generated by the protocol, 30% of structures had a global fold with consistently superimposible regions of regular structure and lower energy terms. The lowest energy candidate of this set was selected as the template for another cycle through the dynamics and annealing protocol, again with randomized starting trajectories. All 20 structures generated at this pass contained a conserved region of defined structure which was superimposible for backbone atoms with a root mean square degree of fit less than 0.8 Å relative to the lowest energy structure. Potential hydrogen-bonded interactions were assessed using INSIGHT and compared with observed deuteron exchange data. Hydrogen bond constraints were added to the NOE-derived constraint table for Ala 11, Leu 16, Tyr 17, and Gly 18, and the XPLOR protocol was reapplied. Hydrogen bond constraints were not added for Lys 25 and Thr 29 as there was insufficient information to establish likely connectivities for hydrogen bonding. A more thorough minimization procedure was then applied for the refinement of all structures. This consisted of 10 000 steps of energy minimization under a more extensive force field with a reduced weighting of the NOE constraint term. Nonbonded interactions were governed by an electrostatic term and a van der Waals (vdW) term represented by a Lennard-Jones potential energy function in the CHARMM force field. All structures were then assessed for energy values and distance violations. No NOE violations greater than 0.3 Å from the constraint range were recorded. Superimpositions of the conserved regions were again performed in INSIGHT.

A series of 20 structures was generated from 67 NOE connectivities recorded for NKA. The above protocol was applied but from a single template starting structure generated randomly within XPLOR from the peptide primary sequence.

DISCUSSION

For the N-teminal region of NPK from Asp 3 to Gly 20, there are sufficient NOE connectivities to define a convergent set of structures with a similar global fold when the simulated annealing protocol is applied. Figure 3 shows structures with backbones superimposed from residue 3 to 18. The predicted helical region, apparent from a qualitative analysis of the NOE data, is confirmed in the quantitative structure calculations. Pairwise RMSD calculated for backbone atoms for residues 3–18 for all 20 refined structures ranged from 0.3 to 1.35 Å, with a mean value of 0.68 Å and a standard deviation of 0.26 Å. Over the entire molecule, pairwise RMSD ranged from 1.92 to 5.73 Å, with a mean value of 3.54 Å and standard deviation of 0.71 Å.

Ramachandran plots of dihedral angles for the helical region indicated that backbone angles are within the allowed ranges.

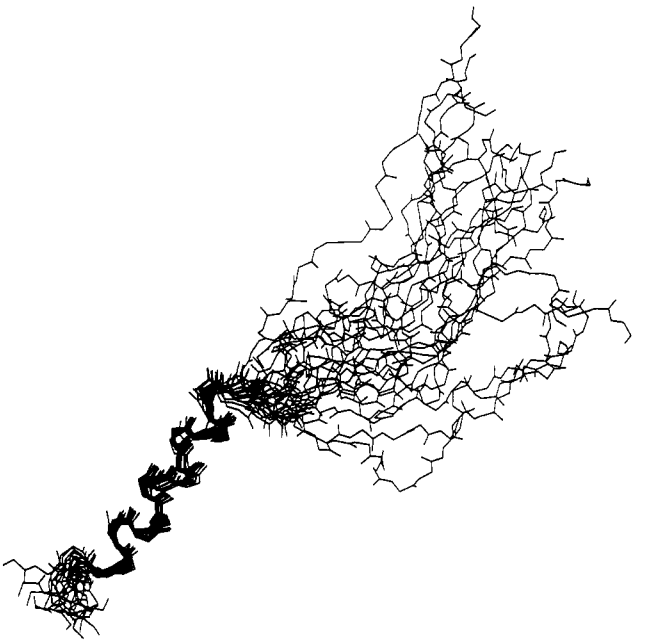

FIGURE 3: Backbone superimpositions for 20 NPK structures generated within the XPLOR protocol. Pairwise RMSD for backbone atoms compared to the lowest energy structure ranges from 0.5 to 0.8 Å.

Interestingly, the experimentally observed coupling constants in this region were all in the range 6.0–8.0 Hz, rather than <5.0 Hz, which is more characteristic of helical structure. Correction of the measured couplings for the influence of line shape still did not yield the characteristically low values associated with a helix, and it may therefore be concluded that the observed couplings are affected by some degree of conformational averaging. The susceptibility of couplings to such averaging is well established (Dyson & Wright, 1991), and, in general, couplings may be considered a less reliable indicator of structure than NOE and amide exchange data.

The good fit of the experimental NOE constraints to the derived helical structure gives confirmation that a well-defined helix is present, the intermediate coupling values perhaps providing a caution that some degree of conformational flexibility is present. The method derived by Bradley *et al.* (1990) was used to estimate the proportion of the conformational ensemble that is in helical form. The equation assumes a two-state model of helical and extended forms interconverting, and a fraction is then calculated from the ratio of $d_{NN}/d_{\alpha N}$ $(i-(i+1))$ NOE intensities to give a percentage value of helix population. For the putative helical region of NPK, the average helicity was calculated to be 89 ± 19%.

As helices in proteins often exhibit well-defined groups of hydrophobic residues upon a single side of the helix, which can be important in interhelix or intermolecular binding interactions, it was of interest to examine the consequences of the derived helical arrangement on the relative displacement of different residue types within the primary sequence. Figure 4 shows a helical wheel plot for the helical region based on hydropathic scores for each residue (Kyte & Doolittle, 1982). It can be seen that a ridge of hydrophobic residues lines the entire length of the helix and that the helix is amphipathic in nature.

While the N-terminal end of NPK clearly displays well-defined secondary structure, Figure 3 shows considerable scatter in the C-terminal half of the molecule. For much of the latter half of NPK, there are too few distance constraints to define any convergent set of coordinates. Many sequential

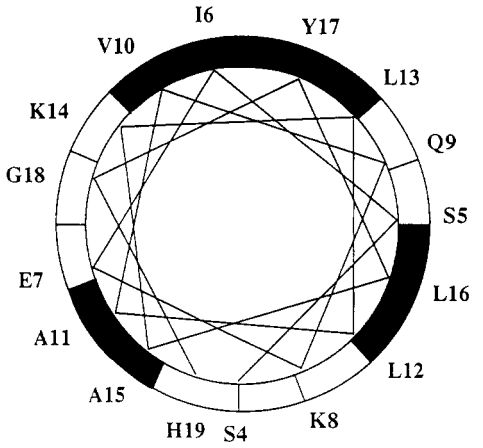

FIGURE 4: Helical wheel representation of NPK_{3-19} showing the helix viewed along its axis. The relative position of the amino acid side chains is indicated by the position on the circumference of the circle, and hydrophobic residues are shaded black.

H^N_i–H^N_{i+1} connectivities are observed for this region, which is potentially indicative of a loose coiling (Sonnichsen *et al.*, 1992), but in the absence of more medium-range connectivities this is insufficient to suggest that a defined helix is present in the C-terminus (Dyson & Wright, 1991). It is the C-terminal part of NPK which shares sequence homology with NKA, and so it was of interest to compare the structure calculations for NPK with those for NKA.

Structures were generated for NKA on the basis of NOESY data recorded at 298 K and 600 MHz in 28% TFE-d_3. Statistical analysis yielded pairwise RMSD for all backbone atoms ranging from 0.96 to 4.85 Å, with a mean value of 2.88 Å and standard deviation of 0.73 Å. N-terminal residues His 1 and Lys 2 had spin systems with crosspeaks greatly reduced in intensity due to motional averaging, and little information was available for this terminus. This is reflected in the observed structures, where root mean square fits for backbone atoms were best for the region 3–10. The global fold was similar for 90% of structures generated from NOE data alone on the first pass through the simulated annealing protocol. No NOE violations greater than 0.1 Å from the constraint distances were observed.

Figure 5 shows a stereo representation of 12 low-energy conformations of NKA with backbone atoms superimposed from residue 3 to 10. While there is some suggestion of a loose helical arrangement in these structures, the number of NOEs is too small to justify a firm conclusion. Rather, it is likely that the structures involve an ensemble of turnlike elements in rapid equilibrium (Osterhout *et al.*, 1989). The set of structures shown in Figure 5 would, in this case, not represent a true structure but a time-averaged approximation to it. This finding is consistent with previous studies of NKA in other solvents. Spectra of NKA obtained in water alone contain little indication of the presence of a defined solution conformation (Chassaing *et al.*, 1986). However, in methanol (Chassaing *et al.*, 1986) and in the 28% TFE-d_3 used in these studies, greater evidence of structural ordering is observed, with more d_{NN} connectivities identified. TFE is a known promoter of secondary structure formation but only where such a propensity exists within the amino acid sequence itself (Sonnichsen *et al.*, 1992), and thus these observations could be relevant to the proposed mode of interaction with the receptor.

Turns are considered among the most basic initiators of protein folding and can promote the formation of regular helix upon addition of small amounts of TFE (Dyson & Wright, 1991). Some stabilization of folding for NKA in TFE-d_3 is observed in the current study, but the observed NOEs are clearly still representative of an averaged ensemble of structural elements, and it is possible that the peptide is simply too short to stabilize a regular helix. A recent study of short peptide

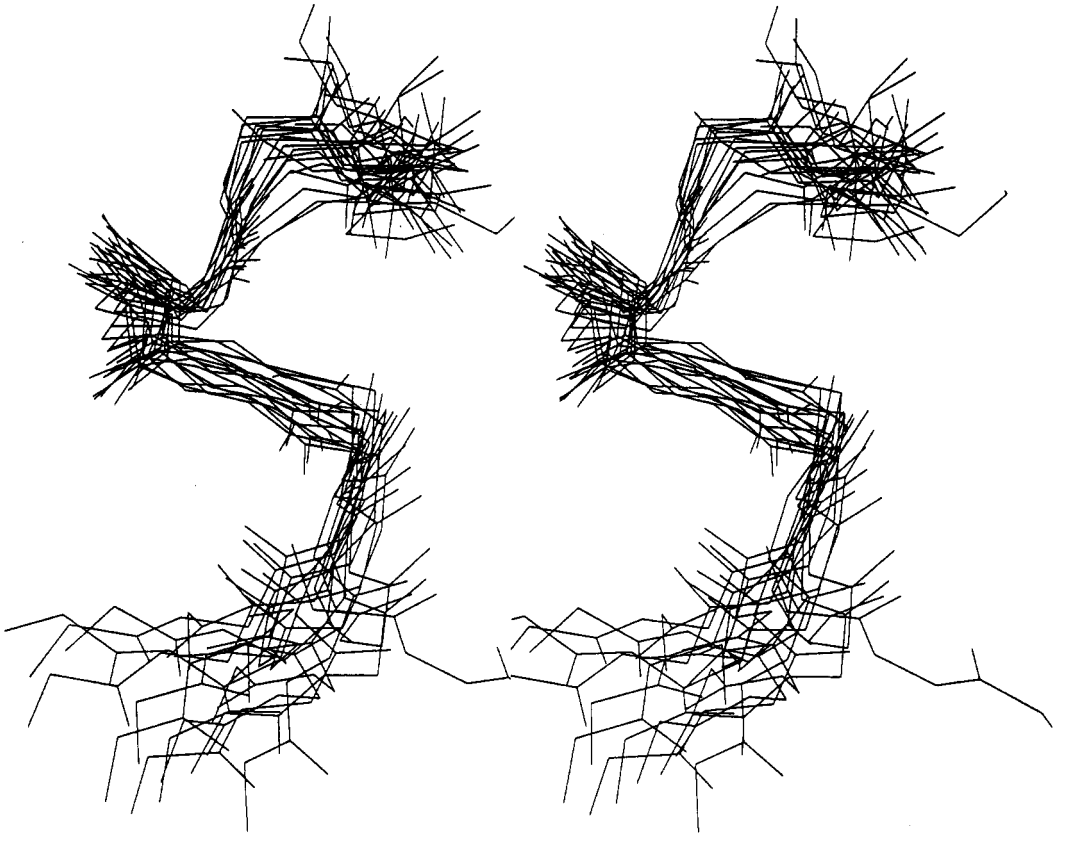

FIGURE 5: Stereo representation of 10 NKA structures superimposed from region 3 to 10, generated by XPLOR, from NOE distance constraints.

fragments of helical regions of proteins suggested that 18 residues may be a lower limit for formation of a fully characterized α-helix (McLean *et al.*, 1991). This limit may be reduced in membrane-like environments, as recent studies in our laboratory have identified a regular α-helix in a 13-residue peptide sequestered within sodium dodecyl sulphate micelles (McLeish *et al.*, 1993) and circular dichroism studies of some tachykinins also in SDS indicate the presence of helix (Woolley & Deber, 1987).

The finding of ensemble averages with some helical stabilization under appropriate solvent conditions in NKA may be compared with the data for NPK. For this peptide the propensity for helix formation is clearly greatest in the N-terminal domain, which in 28% TFE-d_3 forms a well-defined helix. Only a few sequential connectivities between backbone amide protons occur for the C-terminal half of the sequence. These connectivities do not appear in spectra recorded in water solution alone but are readily apparent upon addition of TFE. The size of NPK is more than sufficient to allow stabilization of a regular helix, yet helix formation does not occur in this region of the peptide. It would apear that while there is some propensity for helix in the C-terminal region of NPK, this is no greater than the weak helical tendency seen in NKA itself. Direct comparison between the two NOE schemes for the homologous peptide sequences and their respective chemical shift values indicates that there are no significant differences.

Both peptides rely upon an appropriate solvent environment to adopt secondary structure, and it is with this in mind that we consider possible mechanisms for the improved selectivity of NPK at the NK-2 receptor. It is possible that the large region of defined secondary structure in the N-terminus of NPK holds the key to its enhanced potency. The NK-2 receptor sequence has been determined and has been identified as one of the rhodopsin-like receptors with seven α-helical transmembrane domains (Masu *et al.*, 1987). Interaction of the amphipathic helical region of NPK with helical regions of the NK-2 receptor may facilitate presentation of the NKA homologue to the putative active site. Thus a greater affinity of ligand for receptor may be achieved. Such a suggestion requires no knowledge of the bound conformation of NKA or the corresponding "active" end of NPK but implicitly assumes that their conformations at the receptor would be similar. However, because of the relative lack of structural definition in NKA and the C-terminus of NPK in solution, it cannot be ruled out that there is also the possibility of a discrete difference in the binding conformations of NKA and NPK_{26-36}.

ACKNOWLEDGMENT

We are grateful to Mr. Murray Coles and Mr. Jeff Dyason for their assistance with the structure calculation software implementation and many helpful discussions.

SUPPLEMENTARY MATERIAL AVAILABLE

Two figures indicating the sequential amide connectivities for NPK and NKA in 28% TFE-d_3, both taken from the 250-ms NOESY experiments at 600 MHz and 298 K and 500 MHz and 278 K, respectively (2 pages). Ordering information is given on any current masthead page.

REFERENCES

Beaujouan, J.-C., Saffroy, M., Petitet, F., Torrens, Y., & Glowinski, J. (1988) *Eur. J. Pharmacol. 151*, 353–354.

Bothner-By, A. A., Stephens, R. L., Lee, J., Warren, C. D., & Jeanloz, R. W. (1984) *J. Am. Chem. Soc. 106*, 811.

Bradley, E. K., Thomason, J. F., Cohen, F. E., Kosen, P. A., & Kuntz, D. (1990) *J. Mol. Biol. 215*, 607–622.

Brooks, B. R., Broccolei, R. E., Olafson, B. D., States, D. I., Swaminatham, S., & Karplus, M. (1983) *J. Comput. Chem. 4*, 187–217.

Brunger, A. T. (1992) *XPLOR Manual*, Yale University, New Haven, CT.

Brunger, A. T., Clore, G. M., Gronenborn, A. M., & Karplus, M. (1986) *Proc. Natl. Acad. Sci. U.S.A. 83*, 3801–3805.

Chassaing, G., Convert, O., & Lavielle, S. (1987) in *Peptides 1986, Proceedings of the 19th European Peptide Symposium*, (Theoropoulos, D., Ed.) pp 301–306, Walter de Gruyter & Co., Berlin.

Davis, D. G., & Bax., A. (1985) *J. Magn. Reson. 64*, 533–535.

Driscoll, P. C., Clore, G. M., Beress, L., & Gronenborn, A. M. (1989) *Biochemistry 28*, 2178–2187.

Dyson, H. J., & Wright, P. E. (1991) *Annu. Rev. Biophys. Biophys. Chem. 20*, 519–538.

Griesinger, C., Sorenson, O. W., & Ernst, R. R. (1987) *J. Magn. Reson. 75*, 474–492.

Griesinger, C., Otting, G., Wuthrich, K., & Ernst, R. R. (1988) *J. Am. Chem. Soc. 110*, 7870–7872.

Hanley, M. R, & Jackson, T. (1987) *Nature 329*, 766–767.

Helke, C. J., Krause, J. E., Mantyh, P. W., Couture, R., & Bannon, M. J. (1990) *FASEB J. 4*, 1606–1615.

Henry, J. L., Couture, R., Cuello, A. C., Pelletier, G., Quirion, R., Regoli, D., Eds. (1987) *Substance P and Neurokinins*, Springer-Verlag, New York.

Holzemann, G. (1989) *Kontakte (Darmstadt) 2*, 3–12.

Kumar, A., Ernst, R. R., & Wuthrich, K. (1980) *Biochem. Biophys. Res. Commun. 64*, 2229–2246.

Kyte, J., & Doolittle, R. F. (1982) *J. Mol. Biol. 157*, 105–132.

Levian-Teitelbaum, D., Kolodny, N., Chorev, M., Selinger, Z., & Gilon, C. (1989) *Biopolymers 28*, 51–64.

Loeuillet, D., Convert, O., Lavielle, S., & Chassaing, G. (1989) *J. Pep. Protein Res. 33*, 171–180.

Masu, Y., Nakayama, K., Tamaki, H., Harada, Y., Kuno, M., & Nakanishi, S. (1987) *Nature 329*, 836–838.

McLean, L. R., Hagaman, K. A., Owen, T. J., Krstenansky, J. L. (1991) *Biochemistry 30*, 31–37.

McLeish, M. J., Nielsen, K. J., Wade, J. D., & Craik, D. J. (1993) *FEBS Lett. 315*, 323–328.

Nawa, H., Hirose, T., Takashima, H., Inayama, S., & Nakanishi, S. (1983) *Nature 306*, 32–36.

Nilges, M., Clore, G. M., & Gronenborn, A. M. (1988) *FEBS Lett. 239*, 129–136.

Osterhout, J. J., Jr, Baldwin, R. L., York, E. J., Stewart, J. M., Dyson, H. J., & Wright, P. E. (1989) *Biochemistry 28*, 7059–7064.

Pardi, A., Billeter, M., & Wuthrich, K. (1984) *J. Mol. Biol. 180*, 741–751.

Plateau, P., & Gueron, M. (1982) *J. Am. Chem. Soc. 104*, 7310–7311.

Rance, M., Sorenson, O. W., Bodenhausen, G., Wagner, G., Ernst, R. R., & Wüthrich, K. (1983) *Biochem. Biophys. Res. Commun. 117*, 479–485.

Sonnichsen, F. D., Van Eyk, J. E., Hodges, R. S., & Sykes, B. D. (1992) *Biochemistry 31*, 8790–8798.

Sumner, C. J., Gallagher, K. S., Davis, D. G., Covell, D. G., Jernigan, R. L., & Ferretti, J. A. (1990) *J. Biomol. Struct. Dyn. 8*, 687–707.

Tatemoto, K., Lundberg, J. M., Jornvall, H., & Mutt, V. (1985) *Biochem. Biophys. Res. Commun. 128*, 947–953.

Woolley, G. A., & Deber, C. M. (1987) *Biopolymers 26*, 109–121.

Wuthrich, K. (1986) *NMR of Proteins and Nucleic Acids*, Wiley and Sons, New York.